Rapid Communications

Orbital-free density functional theory correctly models quantum dots when asymptotics, nonlocality, and nonhomogeneity are accounted for

Wenhui Mi* and Michele Pavanello†
Department of Physics, Rutgers University, Newark, New Jersey 07102, USA

(Received 21 November 2018; published 8 July 2019)

Million-atom quantum simulations are in principle feasible with orbital-free density functional theory (OF-DFT) because the algorithms only require simple functional minimizations with respect to the electron density function. In this context, OF-DFT has been useful for simulations of warm dense matter, plasma, cold metals, and alloys. Unfortunately, systems as important as quantum dots and clusters (having highly inhomogeneous electron densities) still fall outside OF-DFT's range of applicability. In this Rapid Communication, we make considerable progress in addressing this century old problem by devising and implementing an accurate, transferable, and universal family of nonlocal noninteracting kinetic energy density functionals that feature correct asymptotics and can handle highly inhomogeneous electron densities. We show that OF-DFT achieves close to chemical accuracy for the electronic energy and reproduces the electron density to about 5% of the benchmark for semiconductor quantum dots and metal clusters. Therefore, this work shows that OF-DFT can reliably simulate systems with highly inhomogeneous electron density, such as clusters and quantum dots, with applicability to the rational design of materials.

DOI: 10.1103/PhysRevB.100.041105

Metal clusters and quantum dots constitute an important class of systems of pivotal importance for materials design, particularly in photovoltaics [1], catalysis [2], and even quantum computing [3]. Although these fields are already strongly shaped by computer-aided design, the high computational cost of available quantum-mechanical methods such as Kohn-Sham density functional theory (KS-DFT) [4,5], arising from the need to build and diagonalize Hamiltonian matrices, is hampering further progress. In this playing field, what is really needed is a breakthrough in techniques alternative to the current standard, and among them [6–12] orbital-free density functional theory (OF-DFT) is a promising candidate.

In OF-DFT, approximating the noninteracting kinetic energy density functional (KEDF, for sake of brevity hereafter we use the acronym KEDF to mean noninteracting KEDF) entirely replaces the need to solve for a Schrödinger equation, completely bypassing its inherent complexity. Particularly, OF-DFT algorithms are promising because they involve a computational scaling of at most $O(N \ln N)$, where N is a measure of the system size, and a memory requirement of only $O(N)$ [13–15].

Unfortunately, even though OF-DFT has already proven to be successful for simulations of million-atom systems involving metals, alloys [15–18], as well as plasmas, warm dense matter [19–21], and also atomic systems [22], its applicability has been severely limited by the accuracy of the available KEDF. For example, systems such as metal clusters and quantum dots have been outside the range of applicability of OF-DFT.

We achieve a breakthrough by carefully balancing three important aspects defining the KEDFs: asymptotics of the corresponding potential, intrinsic nonlocality, and ability to handle nonhomogeneous systems. Thus, already at conception, we make sure that the functionals are nonlocal, that their asymptotics matches the known exact behavior, and that their nonlocal kernels adapt to such large density inhomogeneities as the ones occurring at the interface of nonperiodic systems with the vacuum. For finite systems, such as clusters, the latter is perhaps the most important aspect, which we tackle head on.

In the following, we cast our KEDF development in the current state of the art and derive the main theoretical and algorithmic developments. Afterwards, we benchmark the resulting density functionals by applying them to four metal clusters and four semiconductor quantum dots realized in 100 possible geometries for each, spanning energy windows of several tens of eV.

Over the past two decades there have been tremendous advances in KEDF development [23–40]. The majority of these functionals are appropriate for main-group metallic bulk systems. Some show potential for modeling bulk semiconductors [37,41]. Although semilocal KEDFs [25–27] have seen a recent resurgence [23,24], nonlocal KEDFs such as Wang-Govind-Carter (WGC) [29,30], Huang-Carter (HC) [37], Wang-Teter (WT) [42], Mi-Genova-Pavanello (MGP) [41], and others [31,43,44] have historically delivered better results, particularly for bulk solids. An inspiring study by Chan, Cohen, and Handy found semilocal KEDFs to be theoretically appropriate for applications to clusters [45]. Several works on metallic clusters [46–48] followed [49,50]. The

*Also affiliated with the Department of Chemistry, Rutgers University, Newark, NJ 07102, USA.
†m.pavanello@rutgers.edu; Also affiliated with the Department of Chemistry, Rutgers University, Newark, NJ 07102, USA.

conclusions of those studies were mixed. Thus, in this Rapid Communication, we depart from semilocal KEDFs and adopt fully nonlocal ones exploiting the typical nonlocal KEDF ansatz,

$$T_S[\rho] = T_{TF}[\rho] + T_{vW}[\rho] + T_{NL}[\rho], \tag{1}$$

where T_{TF} is the Thomas-Fermi (TF) KEDF [51,52], $T_{vW}[\rho]$ is the von Weizsäcker (vW) KEDF [53], and $T_{NL}[\rho]$ is the remaining nonlocal contribution. The general form of T_{NL} is

$$T_{NL}[\rho] = \int \rho^{\alpha}(\mathbf{r})\omega_{NL}[\rho](\mathbf{r},\mathbf{r}')\rho^{\beta}(\mathbf{r}')d\mathbf{r}d\mathbf{r}', \tag{2}$$

where $\omega_{NL}[\rho](\mathbf{r},\mathbf{r}')$ is the kernel of the nonlocal KEDF, and α and β are positive scalars.

Let us first describe details of the MGP functional and then outline the developments that extend its applicability to finite systems. Following the lead of Kohn and Sham [54], the starting point of our derivations (common among nonlocal functionals [55]) is the linear response of the free electron gas (i.e., the Lindhard function). The inverse Lindhard function is related to the noninteracting KEDF kernel by two functional integration procedures (Supplemental Material [56], Sec. II). However, this relationship was not exploited until our previous work [41]. Keeping the leading term from a functional integration procedure carried out by parts leads to the WT functional [42], while if the integration is carried out completely, the MGP functional [41] is recovered. MGP's kernel behaves correctly in the low q limit (where the reciprocal space variable q corresponds to $|\mathbf{r}-\mathbf{r}'|$ in a Fourier space defined by the components $e^{iq|\mathbf{r}-\mathbf{r}'|}$) by construction, because we impose the so-called "kinetic electron" (*vide infra*) and therefore it can potentially approach systems beyond bulk metals. In our previous work [41], we found that MGP reproduces with remarkable accuracy the energetic properties and electron densities of silicon and several III-V semiconductors provided that two parameters were adjusted.

The MGP nonlocal potential expression follows from Eq. (1), $v_{MGP}(\mathbf{r}) = v_{TF}(\mathbf{r}) + v_{vW}(\mathbf{r}) + v_{NL}(\mathbf{r})$, and a procedure of functional integration of a suitably defined inverse response function [41] as well as from Eq. (2) constraining $\alpha = \beta = \frac{5}{6}$ [42] (see Sec. II of the Supplemental Material [56]),

$$v_{NL}(\mathbf{r}) = \rho(\mathbf{r})^{-\frac{1}{6}}\hat{F}^{-1}\left[\hat{F}\left[\rho^{\frac{5}{6}}\right](q)\omega_{MGP}(q)\right](\mathbf{r}), \tag{3}$$

where $\hat{F}[\cdot]$ stands for Fourier transform and $\hat{F}^{-1}[\cdot]$ for its inverse. Thus, the inherent approximation in Eq. (3) is that the kernel only depends on the magnitude of $|\mathbf{r}-\mathbf{r}'|$. In particular, the MGP kernel takes the following form,

$$\omega_{MGP}(q) = \omega_{WT}(q) + \omega_{Hyper}(q) + \omega_e(q). \tag{4}$$

The first term, ω_{WT}, is the kernel of the WT functional. The second term, ω_{Hyper}, originates from functional integration. The integration is carried out numerically after an integration by parts (see additional details in Ref. [41]).

The third term, ω_e, is the contribution encoding the kinetic electron which is not originally present in the inverse Lindhard function and needs to be approximated. In the literature, there have been two separate and equivalent discussions about this term: (1) Given the asymptotic behavior of the exchange potential, the Euler equation of DFT imposes an equivalent asymptotic behavior to the noninteracting kinetic energy potential [41]. Such behavior has a $\frac{1}{q^2}$ dependence, where q is the magnitude of the reciprocal space vector. (2) Because the kernel of the noninteracting kinetic energy is related to the inverse Kohn-Sham response function χ_{KS}^{-1} in systems with a gap, this behaves asymptotically as $\frac{1}{q^2}$ [37]. Thus, the ω_e term in the kernel aims at imposing such a known asymptotic behavior.

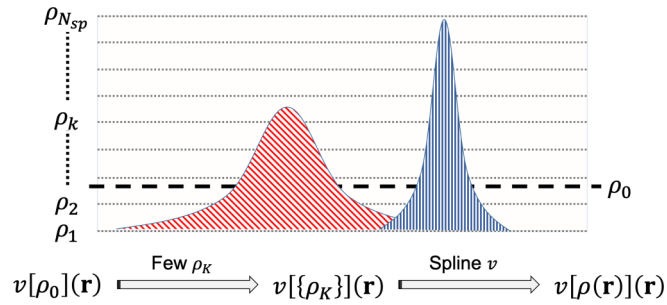

FIG. 1. Two very different electron densities yield the same average density, ρ_0. We propose a generalization of nonlocal KEDFs with a ρ_0-dependent kernel to become dependent on the full $\rho(\mathbf{r})$ by evaluating the potential with a kernel built with $\rho_0 = \rho_k$, $v[\rho_k](\mathbf{r})$, for a set of $\{\rho_k\}_{k\in 1\ldots N_{sp}}$. Afterwards, extend to all possible values of $\rho(\mathbf{r})$ with splines.

We borrow from Ref. [41] the general form of ω_e. However, here we modify it and propose a universal form, containing no adjustable parameters. Namely,

$$\omega_e(q) = \frac{4\pi a}{q^2}\mathrm{erf}^2(q)\exp(-aq^2), \tag{5}$$

where a is a parameter that we relate to the number of electrons, $a = A/N_e^{2/3}$, with $A = 0.2$ and N_e is the total number of electrons. The $N_e^{-\frac{2}{3}}$ dependence is dictated by the $\rho(\mathbf{r})^{\frac{2}{3}}$ dependence of the potential. In this way, the potential goes asymptotically as $\frac{1}{q^2}$ as q approaches small numbers. To avoid numerical inaccuracies, we cap the singularity at $q = 0$ by multiplying with the function $\mathrm{erf}^2(q)$, ensuring smooth behavior as $q \to 0$. The parameter $A = 0.2$ was optimized in test calculations and kept fixed throughout all calculations in this work.

Thus, if the kernel includes $\omega_{WT}(q)$, $\omega_{WT}(q) + \omega_{Hyper}(q)$ or $\omega_{WT}(q) + \omega_{Hyper}(q) + \omega_e(q)$ in Eq. (4), then the corresponding KEDF is called WT, MGP0, or MGP. These kernels are only dependent on the average electron density, $\rho_0 = \frac{N_e}{V}$ (where V is the volume of the simulation cell), through $\eta = q/(2k_F)$, where $k_F = (3\pi^2\rho_0)^{1/3}$ is the Fermi wave vector associated with the average density. This approximation is too strong and is the source reason for needing adjustable parameters in these functionals. In lieu of adjustable parameters, we have made the kernel dependent on the full electron density function $\rho(\mathbf{r})$ instead of ρ_0. In principle, this would benefit and improve the description of systems where the distribution of electron density strongly deviates from uniformity.

Such a strong approximation is shared among most nonlocal functionals. In this Rapid Communication, we propose a method that tackles this limitation and in Fig. 1 we hint

at the proposed workaround. Inspired by the success of the local density approximation (LDA) [57,58], we assume that the potential at a point $\mathbf{r}$ in real space can be approximated by the one of a nonlocal functional evaluated with a kernel $\omega[\rho_0 = \rho(\mathbf{r})](q)$. This is the same principle as LDA applied to nonlocal kernels rather than to the energy densities, as customarily done. Unfortunately, implementing this principle directly would imply a superquadratic computational cost (N nonlocal kinetic potential evaluations each costing $N \ln N$). The computational scaling can be brought back to $O(N \ln N)$ by employing splines. Figure 1 provides a visual depiction of the proposed spline method which we explain below.

A series of ρ_0 values is considered, $\{\rho_k\}$, obtained by dividing the range between 0 and $\rho_{\max} = \max[\rho(\mathbf{r})]$, in equally spaced segments and choosing the total number of k points to be $N_{sp} = 40$. For each ρ_k, there is a corresponding kernel, $\omega_{\mathrm{NL}}(q, \eta(\rho_k))$, that can be tabulated and recovered ahead of computing the potential. Thus, a series of nonlocal potentials is obtained based on Eq. (3), $\{v_{\mathrm{NL}}[\rho_k](\mathbf{r})\}_{k\in 1\ldots N_{sp}}$, and the LDA procedure can be exploited invoking splines,

$$v_{\mathrm{NL}}[\rho(\mathbf{r})](\mathbf{r}) \xleftarrow{\text{spline}} \{v_{\mathrm{NL}}[\rho_1](\mathbf{r}), \ldots, v_{\mathrm{NL}}[\rho_k](\mathbf{r}), \ldots, v_{\mathrm{NL}} \times [\rho_{N_{sp}}](\mathbf{r})\}. \quad (6)$$

This is a scheme for constructing "LDA versions" of MGP (LMGP), WT (LWT) and MGP0 (LMGP0) functionals from the corresponding kernels. Additional details regarding the MGP functional are available in the Supplemental Material Sec. III [56].

Finally, the nonlocal contribution to the total kinetic energy is recovered by a second functional integration [41],

$$T_{\mathrm{NL}}[\rho] = \int d\mathbf{r} \int_0^1 dt\, \rho(\mathbf{r}) v_{\mathrm{NL}}[t\rho](\mathbf{r}). \quad (7)$$

Two other prescriptions for generating density-dependent kernels exist. WGC [30] exploits a Taylor expansion for the kernel around a reasonable value near ρ_0. Unfortunately, this can result in numerical instabilities when the electron density distribution differs much from the one of the free electron gas. Another example is the kernel of the HC functional [37]. It is obtained by solving a differential equation when the electron density is updated. To ameliorate the computational cost, Huang and Carter offer an implementation of HC also featuring a spline technique in the spirit of Soler and coworkers [59].

A major advantage of the LWT and LMGP family of functionals compared to WGC and HC is the fact that they are *universal functionals* with no adjustable parameters. One issue with universal functionals is that they may be weakly transferable. In other words, they may work well for a certain system, but less well for others. In the following, we craft strict and conservative benchmarks for the proposed functionals that show their superiority compared to the current state of the art and their transferability among an array of cluster sizes and types.

To assess this family of KEDFs, we choose random clusters generated by CALYPSO [60–62]. Standard KS-DFT calculations provide benchmark values for the total energy and electron density (KS-DFT employs the exact KEDF) are carried out with QUANTUM ESPRESSO (QE) [63]. OF-DFT simulations are performed with a modified version of ATLAS [64,65] and PROFESS 3.0 [66] which gave the same results. The optimal effective local pseudopotentials (OEPP) [67] are employed for both OF-DFT and KS-DFT calculations. The LDA exchange-correlation functional by Perdew and Zunger [68] is employed in all calculations. Additional technical and computational details are available in the Supplemental Material [56].

With KS-DFT quantities as a reference, we initially select two types of clusters: Mg_8 and Si_8. For each, we compute the total energy of 100 random structures and collect the computed values in Fig. 2. The figure shows a progressive improvement when adopting the functionals WT → MGP → LMGP. Particularly, we note that the consistent bias of MGP (slope differing from KS-DFT) is eliminated by the LDA procedure in LMGP. As shown in the lower insets of Fig. 2, MGP improves dramatically the total energies in comparison with WT. Furthermore, the three parameterless functionals (LWT, LMGP0, and LMGP) are found to outperform their ρ_0-dependent kernel counterparts. We should note that while LWT and LMGP/LMGP0 functionals are universal (no adjustable parameters), MGP results are obtained by adjusting the parameter a independently for Mg_8 and Si_8 clusters ($a = 0.35$ and 0.4, respectively). Strikingly, LMGP values are found to be essentially on top of the KS-DFT results, providing us with an indication that the LDA procedure implemented by splines is stable and accurate.

To confirm the transferability of our functionals, we select six additional cluster systems: Mg_{50}, Si_{50}, Ga_4As_4, $Ga_{25}As_{25}$, and two more Mg_8 (i.e., Mg_8^S and Mg_8^{VS}) featuring shorter average interatomic distances. This set of systems provides us with an array of metallic to semiconducting quantum-dot-like clusters. As shown in Fig. 3, the performance of our functionals is consistent for all systems reproducing total energies across a wide window of energy spanning several eV per atom. In terms of absolute values of total energies, LWT and LMGP0 results are higher and lower than KS-DFT results, respectively. These results are a source of considerable excitement—not only because the LMGP energy values correlate almost perfectly with the KS-DFT benchmark, but more importantly the LDA procedure (which is numerical in nature) is found to be stable for all systems considered. LMGP converges for more than 90% of the structures in all systems with an average convergence rate of over 95%.

To quantify the performance of our functionals, Table I shows the mean unsigned error (MUE) of total OF-DFT energies compared to KS-DFT for the 100 random structures of each system computed with LWT, LMGP, and LMGP0, as well as WT, and TF + $\frac{1}{5}$vW.

An option is to also compare against the Huang-Carter [37] (HC) and the Wang-Govind-Carter (WGC) functionals. However, even though HC is considered to be the most accurate KEDF presently available, it is also known for drawbacks that make it unsuitable for applications to finite systems [35]. Thus, in this work, we compare against the other functionals.

Table I shows that LWT considerably improves over WT. Thus, the LDA procedure improves the corresponding KEDF with a density-independent kernel while at the same time removing the ρ_0 dependence in the functional. Interestingly, LMGP0 performs even better than LWT. This is an indication that the hypercorrelation term in the kernel further

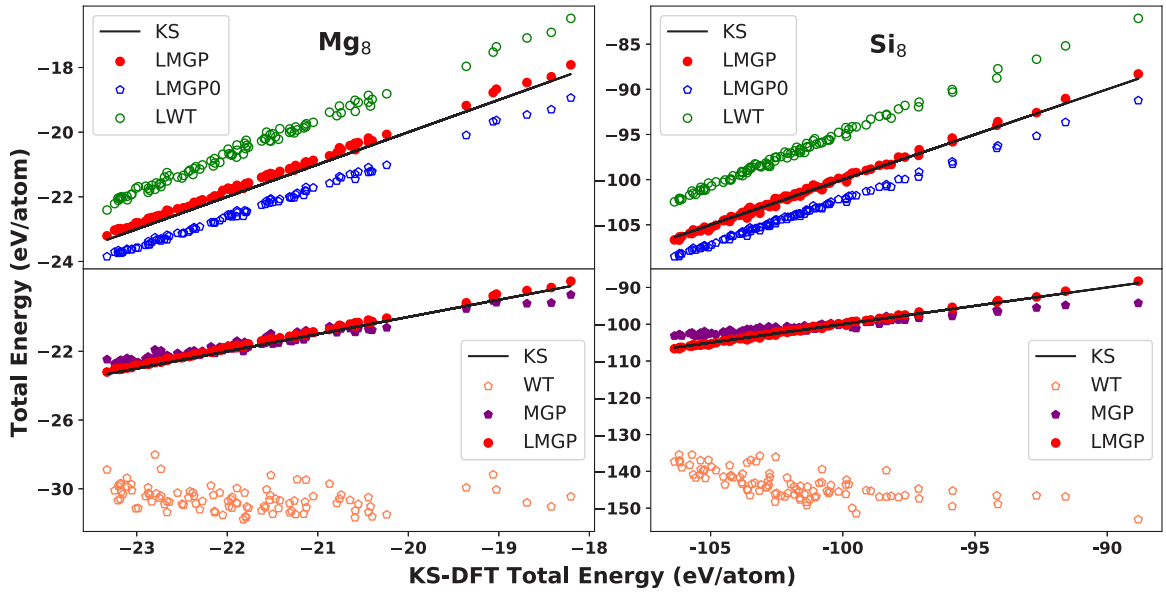

FIG. 2. Total energies computed with WT, MGP, LWT, LMGP0, and LMGP KEDFs compared to reference KS-DFT values (on the diagonal) for 100 random structures of Mg_8 (left) and Si_8 (right) clusters.

improves the performance of the functional. Adding the kinetic electron [i.e., the additional term $\omega_e(q)$ in the kernel, see Eq. (4)], the LMGP functional achieves an additional and important improvement over LMGP0, lining itself up to the KS-DFT results in an almost quantitative fashion. Strikingly, this is so despite the relatively uncomplicated formalism for the kinetic electron term in Eq. (5). Scatter plots of the OF-DFT to KS-DFT deviations are available in Fig. S1 of the Supplemental Material [56] and similar plots to Figs. 2 and 3 for the value of just the KEDF are available in Fig. S2.

To address questions related to the possible fortuitous agreement between OF-DFT and KS-DFT, in the Supplemental Material [56], we show in Figs. S3 and S4 that LMGP predicts excellent atomic electron densities and KEDF potentials for He, Mg, Si, Ga, and As. Figure S2 shows that, similarly to the total energy, the KEDF values obtained by LMGP also are in excellent agreement (similar deviation to the total energy results presented above) with the exact KS-DFT values. Tables S1 and S2 summarize test calculations showing that LMGP also correctly predicts the energy difference between the clusters of different composition as well as equilibrium geometries for the clusters and the forces in the vicinity of the equilibrium geometry.

Reproducing the electron density is as important as reproducing the total energy [69]. Thus, we define $\frac{1}{2N_e}\int|\rho_{\text{OF-DFT}}(\mathbf{r})-\rho_{\text{KS-DFT}}(\mathbf{r})|d\mathbf{r}$, a measure of the electron density difference between KS-DFT and OF-DFT. The performances of the various functionals in reproducing the KS-DFT electron density are listed in Table I. Once again, our three functionals constitute an improvement over TF + $\frac{1}{5}$vW and WT functionals.

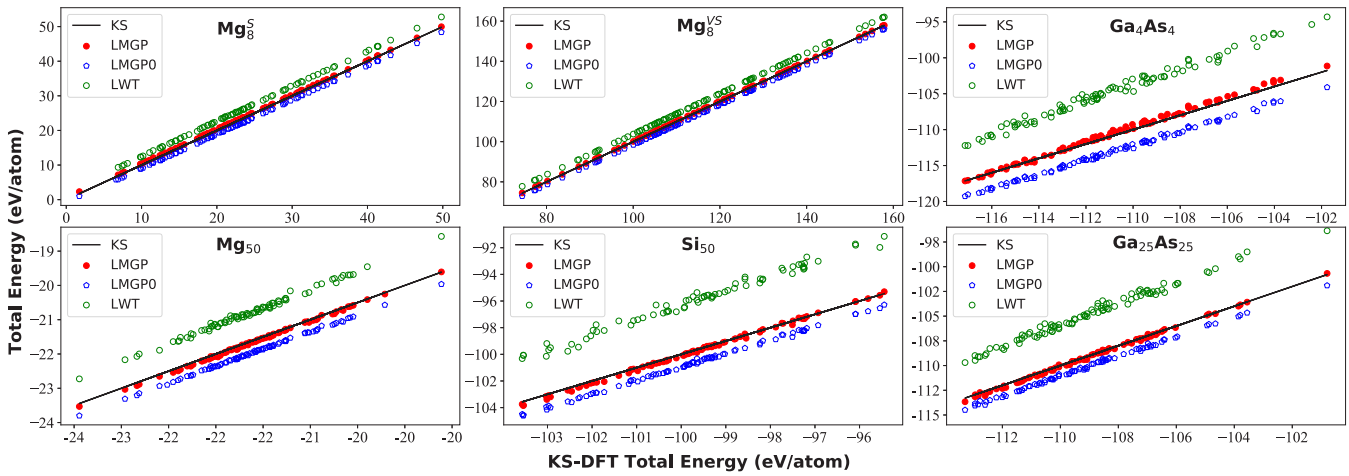

FIG. 3. The total energies obtained by OF-DFT employing LWT, LMGP0, and LMGP KEDFs in comparison with the reference KS-DFT results for six different cluster systems, Mg_{50}, Si_{50}, Ga_4As_4, $Ga_{25}As_{25}$, and two Mg_8 systems with shorter average bond distances: Mg_8^S (i.e., strained) and Mg_8^{VS} (i.e., very strained), respectively. For each system we generate 100 random structures.

TABLE I. Mean unsigned error (MUE) for the total energy in eV/atom and mean unsigned relative error (MURE) for the electron density in percentage points (in parentheses) compared to KS-DFT. Superscripts S and VS stand for "strained" and "very strained," respectively.

Systems	LMGP	LMGP0	LWT	TF + $\frac{1}{5}$vW	WT
Mg_8	0.18 (3.79)	0.63 (4.12)	1.19 (4.05)	1.09 (11.36)	8.79 (16.0)
Si_8	0.22 (4.84)	2.17 (4.90)	4.86 (4.74)	1.46 (8.28)	41.7 (17.5)
Ga_4As_4	0.34 (5.40)	2.21 (5.43)	6.15 (4.89)	1.55 (8.94)	51.8 (19.3)
Mg_{50}	0.05 (3.31)	0.35 (3.42)	0.84 (2.38)	0.95 (9.56)	3.23 (10.3)
Si_{50}	0.11 (4.59)	0.95 (4.65)	3.73 (3.60)	1.53 (7.24)	16.4 (14.2)
$Ga_{25}As_{25}$	0.13 (5.21)	1.06 (5.26)	4.29 (3.19)	1.67 (7.79)	22.7 (16.8)
Mg_8^S	0.28 (5.20)	1.16 (5.34)	2.66 (5.29)	0.27 (7.63)	19.4 (18.6)
Mg_8^{VS}	0.09 (3.94)	1.67 (4.10)	3.88 (4.87)	0.10 (5.60)	24.0 (17.5)

We point out that although the total energies computed by TF+$\frac{1}{5}$vW only partially differ from LWT, the LWT electron density is of much higher quality than the one from TF+$\frac{1}{5}$vW.

In conclusion, we have made considerable steps forward towards addressing a long-standing problem in the field of OF-DFT, i.e., the simulation of finite systems, such as quantum dots. Our method reproduces benchmark KS-DFT results with unprecedented accuracy for a pure KEDF. Thus, this constitutes a major step forward for OF-DFT, a framework that was thought to only be reliably applicable to bulk metals and alloys. Quantum dot structure prediction is now feasible with OF-DFT, opening the door to a different regime of applicability for this method.

Our results are achieved by (1) imposing correct asymptotic behavior of the KE potentials, (2) accounting for nonlocality in the functional by construction, and (3) allowing the functional to adapt to systems with a highly inhomogeneous electron density, via a technique inspired by the LDA approximation. Such a comprehensive yet simple prescription leads to a numerically stable family of KEDFs which we apply to eight different quantum dots, each realized in 100 different structures spanning energy windows ranging between 10 and 80 eV. Our most refined functional, LMGP, consistently reproduces the KS-DFT electronic energy for all 50-atom quantum dots to within 130 meV/atom. The energies of the 8-atom clusters are within 340 meV/atom of the KS-DFT reference. These errors are for the most part systematic in nature, as the OF-DFT energy values correlate almost perfectly to the KS-DFT benchmarks.

Although the KEDFs presented here predict with unprecedented accuracy the total energy and electron density of the considered quantum dots, there is still room for improvement both in terms of computational accuracy as well as efficiency. Particularly, LMGP shows a significant improvement in comparison to LWT in terms of total energies, but struggles to improve the quality of the electron density. This indicates that the simple LDA approximation for the kernels can be further improved, for instance, by including a dependency over the density gradient. This is currently being investigated.

This material is based upon work supported by the National Science Foundation under Grant No. CHE-1553993. We thank Chuck Witt for the useful feedback on our manuscript.

[1] X. Lan, S. Masala, and E. H. Sargent, Nat. Mater. **13**, 233 (2014).
[2] E. C. Tyo and S. Vajda, Nat. Nanotechnol. **10**, 577 (2015).
[3] Y. H. Huo, B. J. Witek, S. Kumar, J. R. Cardenas, J. X. Zhang, N. Akopian, R. Singh, E. Zallo, R. Grifone, D. Kriegner, R. Trotta, F. Ding, J. Stangl, V. Zwiller, G. Bester, A. Rastelli, and O. G. Schmidt, Nat. Phys. **10**, 46 (2013).
[4] N. T. Maitra, J. Chem. Phys. **144**, 220901 (2016).
[5] K. Burke, J. Chem. Phys. **136**, 150901 (2012).
[6] T. J. Giese and D. M. York, J. Phys.: Condens. Matter **29**, 383002 (2017).
[7] J. VandeVondele, U. Borštnik, and J. Hutter, J. Chem. Theory Comput. **8**, 3565 (2012).
[8] A. Krishtal, D. Sinha, A. Genova, and M. Pavanello, J. Phys.: Condens. Matter **27**, 183202 (2015).
[9] W. Yang, Phys. Rev. Lett. **66**, 1438 (1991).
[10] C. R. Jacob and J. Neugebauer, WIREs: Comput. Mol. Sci. **4**, 325 (2014).
[11] D. G. Fedorov, WIREs: Comput. Mol. Sci. **7**, e1322 (2017).
[12] S. Goedecker, Rev. Mod. Phys. **71**, 1085 (1999).
[13] T. A. Wesolowski and Y. A. Wang, *Recent Progress in Orbital-Free Density Functional Theory*, Recent Advances in Computational Chemistry Vol. 6 (World Scientific, Singapore, 2013).
[14] V. V. Karasiev and S. B. Trickey, Comput. Phys. Commun. **183**, 2519 (2012).
[15] W. C. Witt, G. Beatriz, J. M. Dieterich, and E. A. Carter, J. Mater. Res. **33**, 777 (2018).
[16] X. Shao, Q. Xu, S. Wang, J. Lv, Y. Wang, and Y. Ma, Comput. Phys. Commun. **233**, 78 (2018).
[17] L. Hung and E. A. Carter, Chem. Phys. Lett. **475**, 163 (2009).
[18] D. J. González, L. E. González, and M. J. Stott, Phys. Rev. Lett. **92**, 085501 (2004).
[19] T. G. White, S. Richardson, B. J. B. Crowley, L. K. Pattison, J. W. O. Harris, and G. Gregori, Phys. Rev. Lett. **111**, 175002 (2013).
[20] Y. H. Ding, A. J. White, S. X. Hu, O. Certik, and L. A. Collins, Phys. Rev. Lett. **121**, 145001 (2018).
[21] T. Sjostrom and J. Daligault, Phys. Rev. Lett. **113**, 155006 (2014).

[22] H. Levamaki, Á. Nagy, K. Kokko, and L. Vitos, Phys. Rev. A **92**, 062502 (2015).
[23] L. A. Constantin, E. Fabiano, and F. Della Sala, J. Phys. Chem. Lett. **9**, 4385 (2018).
[24] K. Luo, V. V. Karasiev, and S. B. Trickey, Phys. Rev. B **98**, 041111(R) (2018).
[25] V. V. Karasiev and S. B. Trickey, *Advances in Quantum Chemistry* (Elsevier, Amsterdam, 2015), pp. 221–245.
[26] S. B. Trickey, V. V. Karasiev, and R. S. Jones, Int. J. Quantum Chem. **109**, 2943 (2009).
[27] V. V. Karasiev, R. S. Jones, S. B. Trickey, and F. E. Harris, Phys. Rev. B **80**, 245120 (2009).
[28] V. V. Karasiev, D. Chakraborty, O. A. Shukruto, and S. B. Trickey, Phys. Rev. B **88**, 161108(R) (2013).
[29] Y. A. Wang, N. Govind, and E. A. Carter, Phys. Rev. B **58**, 13465 (1998).
[30] Y. A. Wang, N. Govind, and E. A. Carter, Phys. Rev. B **60**, 16350 (1999).
[31] F. Perrot, J. Phys.: Condens. Matter **6**, 431 (1994).
[32] S. Laricchia, L. A. Constantin, E. Fabiano, and F. Della Sala, J. Chem. Theory Comput. **10**, 164 (2014).
[33] S. Smiga, E. Fabiano, L. A. Constantin, and F. D. Sala, J. Chem. Phys. **146**, 064105 (2017).
[34] J.-D. Chai and J. D. Weeks, Phys. Rev. B **75**, 205122 (2007).
[35] J. Xia and E. A. Carter, Phys. Rev. B **86**, 235109 (2012).
[36] J. Xia, C. Huang, I. Shin, and E. A. Carter, J. Chem. Phys. **136**, 084102 (2012).
[37] C. Huang and E. A. Carter, Phys. Rev. B **81**, 045206 (2010).
[38] G. S. Ho, V. L. Lignères, and E. A. Carter, Phys. Rev. B **78**, 045105 (2008).
[39] B. Zhou, V. L. Lignères, and E. A. Carter, J. Chem. Phys. **122**, 044103 (2005).
[40] K. M. Carling and E. A. Carter, Modell. Simul. Mater. Sci. Eng. **11**, 339 (2003).
[41] W. Mi, A. Genova, and M. Pavanello, J. Chem. Phys. **148**, 184107 (2018).
[42] L.-W. Wang and M. P. Teter, Phys. Rev. B **45**, 13196 (1992).
[43] M. Pearson, E. Smargiassi, and P. A. Madden, J. Phys.: Condens. Matter **5**, 3221 (1993).
[44] E. Smargiassi and P. A. Madden, Phys. Rev. B **49**, 5220 (1994).
[45] G. K.-L. Chan, A. J. Cohen, and N. C. Handy, J. Chem. Phys. **114**, 631 (2001).
[46] A. Aguado, Phys. Rev. B **63**, 115404 (2001).
[47] A. Aguado, J. M. López, J. A. Alonso, and M. J. Stott, J. Phys. Chem. B **105**, 2386 (2001).
[48] A. Aguado, J. M. López, J. A. Alonso, and M. J. Stott, J. Chem. Phys. **111**, 6026 (1999).
[49] G. S. Ho, C. Huang, and E. A. Carter, Curr. Opin. Solid State Mater. Sci. **11**, 57 (2007).
[50] A. Aguado, D. J. González, L. E. González, J. M. López, S. Núñez, and M. J. Stott, *Recent Progress in Orbital-Free Density Functional Theory* (Ref. [13]), pp. 55–145.
[51] E. Fermi, Rend. Accad. Naz. Lincei **6**, 602 (1927).
[52] L. A. Thomas, Proc. Cambridge Philos. Soc. **23**, 542 (1927).
[53] C. F. von Weizsäcker, Z. Phys. **96**, 431 (1935).
[54] W. Kohn and L. J. Sham, Phys. Rev. **140**, A1133 (1965).
[55] Y. A. Wang and E. A. Carter, in *Theoretical Methods in Condensed Phase Chemistry*, edited by S. D. Schwartz (Kluwer, Dordrecht, 2000), pp. 117–184.
[56] See Supplemental Material at http://link.aps.org/supplemental/10.1103/PhysRevB.100.041105 for additional tables and figures.
[57] D. M. Ceperley and B. J. Alder, Phys. Rev. Lett. **45**, 566 (1980).
[58] J. P. Perdew and Y. Wang, Phys. Rev. B **45**, 13244 (1992).
[59] G. Román-Pérez and J. M. Soler, Phys. Rev. Lett. **103**, 096102 (2009).
[60] Y. Wang, J. Lv, L. Zhu, and Y. Ma, Comput. Phys. Commun. **183**, 2063 (2012).
[61] Y. Wang, J. Lv, L. Zhu, and Y. Ma, Phys. Rev. B **82**, 094116 (2010).
[62] J. Lv, Y. Wang, L. Zhu, and Y. Ma, J. Chem. Phys. **137**, 084104 (2012).
[63] P. Giannozzi, S. Baroni, N. Bonini, M. Calandra, R. Car, C. Cavazzoni, D. Ceresoli, G. L. Chiarotti, M. Cococcioni, I. Dabo, A. Dal Corso, S. de Gironcoli, S. Fabris, G. Fratesi, R. Gebauer, U. Gerstmann, C. Gougoussis, A. Kokalj, M. Lazzeri, L. Martin-Samos *et al.*, J. Phys.: Condens. Matter **21**, 395502 (2009).
[64] W. Mi, X. Shao, C. Su, Y. Zhou, S. Zhang, Q. Li, H. Wang, L. Zhang, M. Miao, Y. Wang, and Y. Ma, Comput. Phys. Commun. **200**, 87 (2016).
[65] X. Shao, W. Mi, Q. Xu, Y. Wang, and Y. Ma, J. Chem. Phys. **145**, 184110 (2016).
[66] M. Chen, J. Xia, C. Huang, J. M. Dieterich, L. Hung, I. Shin, and E. A. Carter, Comput. Phys. Commun. **190**, 228 (2015).
[67] W. Mi, S. Zhang, Y. Wang, Y. Ma, and M. Miao, J. Chem. Phys. **144**, 134108 (2016).
[68] J. P. Perdew and A. Zunger, Phys. Rev. B **23**, 5048 (1981).
[69] M. G. Medvedev, I. S. Bushmarinov, J. Sun, J. P. Perdew, and K. A. Lyssenko, Science **355**, 49 (2017).